

Metal Borohydrides

Inclusion of Neon into an Yttrium Borohydride Structure at Elevated Pressure – An Experimental and Theoretical Study

Tomasz Jaroń,^{*,[a,b]} Agnieszka Starobrat,^[a,c] Viktor V. Struzhkin,^[d] and Wojciech Grochala^[a]

This work is dedicated to Prof. T. M. Krygowski on the occasion of his 80th birthday.

HPSTAR
985-2020

Abstract: We report here the experimental and computational results of a high-pressure study (up to 40 GPa) of yttrium borohydride. During compression in neon pressure medium the cage-like RuO_3 structure of $\alpha\text{-Y}(\text{BH}_4)_3$ is stabilized by the formation of the inclusion compound with this chemically inert gas. Ne atoms fill the voids available in the crystal structure of the host at the special 0 0 0 and 0.5 0.5 0.5 positions. The inclusion

compound preserves high crystallinity up to ca. 10 GPa, while gradual amorphization is observed at higher pressures. The results of our DFT calculations indicate that although the molecular volumes of the tested system are rather well modeled using PBEsol functional, significant improvement, especially in terms of the phases' relative energy can be made when applying dispersion correction, using PBE-TS approach.

Introduction

The recent extensive research on various borohydrides, motivated predominantly by prospective hydrogen storage, has led to an impressive broadening of knowledge related to this group of compounds.^[1–3] This has been manifested in significant growth of the number of known solvent-free borohydrides, strongly supported by the development of the synthetic methods, in parallel with the structural identification of the products.^[4–11] Besides the storage of hydrogen and their traditional use in reduction processes, borohydrides are studied in the context of solid-state ion conduction,^[12–15] magnetic and luminescent properties,^[16–19] or as porous materials, capable for loading of guest molecules.^[20]

In order to modify the properties of borohydrides related to the above-mentioned areas, several strategies have been employed, like anion or cation substitution (including the formation of mixed-ion compounds^[7,21–25]), catalytic doping,^[26] or nanoconfinement.^[27] Thermal or pressure-induced polymorphism provides other tuning options and can influence the

pathway of hydrogen evolution, as it was reported for the high-temperature phase of yttrium borohydride^[28] or high-pressure phase of ammonia borane.^[29] Several borohydrides, mainly those containing alkali or alkaline earth metals, have been explored under high pressure, which broadened their crystal chemistry and added a second dimension to their phase diagrams.^[30–34] Interestingly, two borohydrides, $\text{Mg}(\text{BH}_4)_2$ and $\text{Mn}(\text{BH}_4)_2$, reveal phase transition around 1 GPa (pressure range easily achievable in a hydraulic press, like laboratory pelletizer, or even during high-energy milling) to the denser δ phases, which are metastable under ambient conditions.^[20,35]

Yttrium borohydride discussed in this work is an example of borohydride of a trivalent metal. Similarly to most of its rare-earth analogs, two polymorphic forms are known, the low-temperature α form and the high-temperature β one.^[36–42] Both are variants of the ReO_3 structure, the prototypical 3D $\text{AX}_6/2$ structure, i.e. the structure containing corner-sharing octahedra forming a 3D lattice (Figure 1). The first coordination sphere of yttrium contains as many as 12 hydride anions (coming from bidentate coordination by six BH_4^- anions), and it is of interest

[a] Dr. T. Jaroń, A. Starobrat, Prof. W. Grochala
Centre of New Technologies, University of Warsaw,
Banacha 2c, 02-097 Warsaw, Poland
E-mail: t.jaron@cent.uw.edu.pl

[b] Dr. T. Jaroń
Geophysical Laboratory, Carnegie Institution of Washington,
5251 Broad Branch Road NW, Washington, DC 20015, United States

[c] A. Starobrat
College of Inter-Faculty Individual Studies in Mathematics and Natural
Sciences (MISMaP), University of Warsaw,
Banacha 2c, 02-097 Warsaw, Poland

[d] Dr. V. V. Struzhkin
Center for High Pressure Science and Technology Advanced Research,
Shanghai, China

Supporting information and ORCID(s) from the author(s) for this article are available on the WWW under <https://doi.org/10.1002/ejic.202000631>.

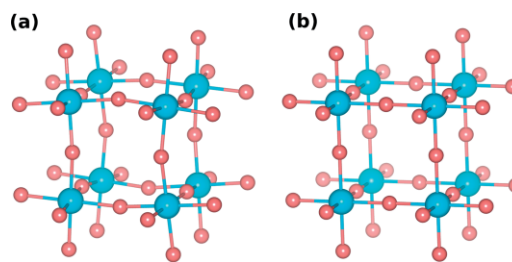


Figure 1. The structure of Y/B sublattice of $\text{Y}(\text{BH}_4)_3$ (the variant of ReO_3 type): (a) $\text{Im}\bar{3}$ – prototypical to $\alpha\text{-Y}(\text{BH}_4)_3$ of $\text{Pa}\bar{3}$ symmetry, (b) $\text{Pm}\bar{3}m$ – prototypical to $\beta\text{-Y}(\text{BH}_4)_3$ of $\text{Fm}\bar{3}c$ symmetry. B – pink, small balls, Y – light blue, large balls.

whether an even higher coordination number could be reached when this compound is compressed at large external pressure.

Here we report on the influence of pressure on α -Y(BH₄)₃, during compression up to ca. 40 GPa. The experiments have been performed using a diamond anvil cell (DAC), while neon was used as a pressure medium. Surprisingly, instead of an increase of the coordination number of a metal center, we observe the stabilization of the cage-like RuO₃ structure by formation of the inclusion compound with chemically inert neon filling the voids in the crystal structure. The inclusion compound preserves high crystallinity up to ca. 10 GPa, while gradual amorphization is observed at higher pressures.

Results and Discussion

The investigated samples contained a mixture of α -Y(BH₄)₃ and LiCl, as synthesized in a mechanochemical process.^[38] Neon, which is probably the most chemically inert noble gas,^[43–45] has been used as the pressure medium. In the in situ diffraction experiments, the diffraction peaks from the sample, pressure standard (Au), and pressure medium were accompanied by a few moderate signals from the unidentified phase, Figure 2. The diffraction signals from α -Y(BH₄)₃ shift to higher 2θ values (lower d) during compression and, simultaneously, their intensity decreases, virtually vanishing at the highest pressure range achieved in our experiments. The diffraction peaks from the crystalline borohydride phase broaden, Figure 2b. We have not detected a clear amorphous halo, however, such observation would be significantly straightened due to the relatively high background level, the presence of other crystalline phases and the rather weak scattering from the sample, Figure S6. Therefore, the diffraction data were analyzed using the Rietveld refinement only up to 17.6 GPa, (cf. Supporting Information, SI), while the lattice parameter of cubic α -Y(BH₄)₃ for higher pressures has been estimated from the measured d values for the strongest (200) reflection. The Rietveld fit reveals rather good conformity to the experimental data obtained under lower pressures, which significantly worsens above 10.3 GPa, due to the increase of the relative background level and the peak broadening. Re-crystallization of the amorphized sample has not been observed during decompression.

Our experimental results indicate that no phase transition occurs, but rather a gradual amorphization is observed when α -Y(BH₄)₃ is compressed in Ne. Recently, Schouwink and Tumanov^[23,46] have reported that α -Y(BH₄)₃ transforms to the orthorhombic *I*bm2 (labeled as HP2 by these authors) phase around 5 GPa, with $c_{\text{HP2}} \approx c_{\alpha}/2$. However, in their experiments, no pressure medium has been used at all. Their experimental setup provided non-hydrostatic compression of the sample, however, no preferred orientation has been observed and the ruby line fluorescence remained well-defined over the whole pressure range studied by these authors. Advantageously, no additional chemical component was introduced to the system in their experiments.

We notice that for pressures of 4 GPa and above, the molecular volumes of α -Y(BH₄)₃ obtained by us are larger by ca. 6 % than those reported for this phase by Schouwink and Tumanov.

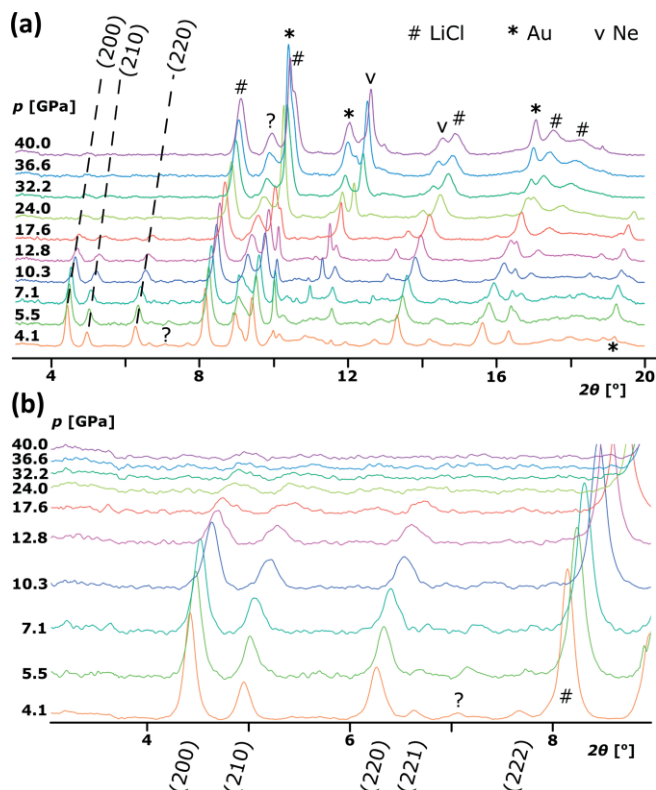


Figure 2. (a) Overview of the diffraction patterns of Y(BH₄)₃ during compression in Ne environment. Several significant low-angle reflections of α -Y(BH₄)₃ have been marked with the dashed lines as an eye-guide. (b) Low-angle range of the patterns. ? – the strongest reflections from an unidentified phase. The background has been subtracted and the patterns have been normalized to the (111) reflection of LiCl on the basis of height.

This difference in molecular volumes is even more pronounced for higher pressures, where the incompletely resolved phase (denoted HP2) was seen in their experiments, (as related to ca. 12 % volume collapse), Figure S2. Nevertheless, the unit cell mentioned by Schouwink et al. clearly does not fit to our diffraction data, Figure S13. These results testify a completely different behavior of Schouwink and Tumanov's, and our samples. The differences are clearly due to the presence of the pressure medium, neon, in our experiments. Thus, the behavior observed here is likely caused by the incorporation of neon into the cage-like crystal structure of α -Y(BH₄)₃ in our experiments.

In order to confirm or refute this hypothesis and understand the discrepancies between the two datasets, we have performed DFT calculations for the viable structures of Y(BH₄)₃ under compression. Although about fifteen monometallic borohydrides of trivalent metals, M^{III}, have been reported^[47] only some of them can serve as usable prototypes in this case. A few compounds can be excluded *a priori*, e.g. volatile Ti(BH₄)₃ with hitherto unknown solid-state structure, and Al(BH₄)₃, which contains too small Al³⁺ cation to serve as a reliable model for potential high-pressure structure of Y(BH₄)₃ (the compounds of lighter elements resemble rather their heavier analogues under compression^[48]). The other M^{III} borohydrides adopt the three types of crystal structures which can be derived from the above-mentioned polymorphs of ReO₃: the borohydrides con-

taining the largest La^{3+} and Ce^{3+} crystallize in $R\bar{3}c$ space group, while for the smaller cations two cubic polymorphs are known: α , $Pa\bar{3}$ and β , $Fm\bar{3}c$.^[36,47] These structures are closely related – they differ in fact by the arrangement of $\text{M}^{\text{III}}(\text{BH}_4)_6$ octahedra and their degree of deformation. Namely, while the $Fm\bar{3}c$ structure is formed by the undistorted $\text{M}^{\text{III}}(\text{BH}_4)_6$ octahedra and $\text{M}^{\text{III}}\text{--B--M}^{\text{III}}$ bridges with an angle of 180° , the former building blocks are tilted in the $R\bar{3}c$ phase which results in bent $\text{M}^{\text{III}}\text{--B--M}^{\text{III}}$ bridges. In the α phase, the octahedra are additionally distorted, Figure 3, which leads to better packing.

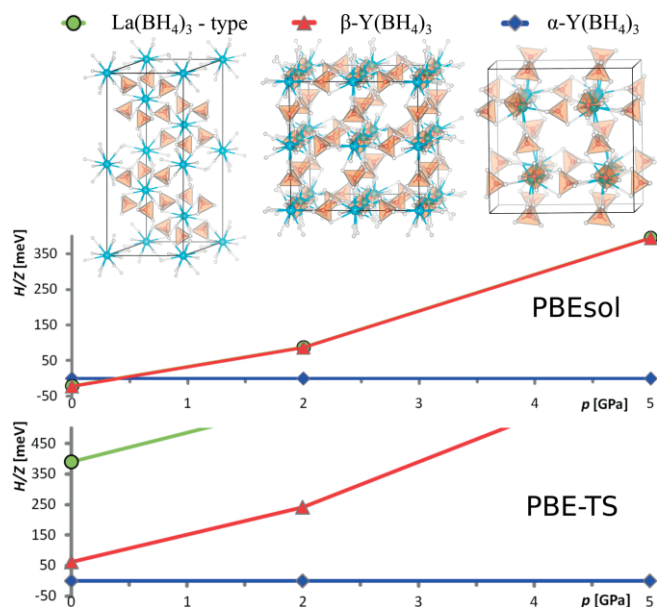


Figure 3. The crystal structures considered in this study (top) and their relative enthalpies calculated using PBEsol functional (middle) and PBE functional with TS dispersion correction (bottom). Note the near-overlap of the $\text{La}(\text{BH}_4)_3$ -type structure and $\beta\text{-Y}(\text{BH}_4)_3$ for PBEsol functional, while their clear separation in PBE-TS approach.

The theoretical results depend on the method applied, Figure 3. The results obtained using PBEsol functional suggest that the β and $\text{La}(\text{BH}_4)_3$ -type phases have virtually the same enthalpy at 0 K in the whole pressure range studied. This is related to the close convergence of the latter phase to the geometry of $\beta\text{-Y}(\text{BH}_4)_3$ of the highest symmetry, with no tilt of $\text{M}^{\text{III}}(\text{BH}_4)_6$ octahedra [contrary to genuine $\text{La}(\text{BH}_4)_3$]. Under ambient pressure, these two phases have slightly more negative enthalpy than $\alpha\text{-Y}(\text{BH}_4)_3$, by a mere 20 meV (corresponding to 1.9 kJ mol^{-1}). Although this is not a lot yet it contradicts the fact that the latter is more stable in the experiment at ambient (p, T) conditions, while the β -form is the high- T one. Such a small discrepancy for $p = 0 \text{ GPa}$ has already been reported^[28,49] and is related to the drawbacks of computational methods applied (PBE and $\text{PW}^{[50]}$ functionals). However, applying the TS dispersion correction to the PBE functional renders $\beta\text{-Y}(\text{BH}_4)_3$ less favored energetically by 61 meV (5.9 kJ mol^{-1}) from the α -form, in agreement with experiment. Also, the $\text{La}(\text{BH}_4)_3$ -type structure now becomes much less favored.

In both methodologies, the $\alpha\text{-Y}(\text{BH}_4)_3$ phase is increasingly stable with respect to other forms as the pressure rises. This is not surprising due to the pronounced better packing of α -

$\text{Y}(\text{BH}_4)_3$, which results in beneficial pV factor under higher pressures [note, the relative difference of calculated molecular volume of the α and β phases of $\text{Y}(\text{BH}_4)_3$ reaches 5 % under ambient pressure, and 19 % under 5 GPa, Tab. S3]. These computational results indicate that α ($Pa\bar{3}$) polymorph of $\text{Y}(\text{BH}_4)_3$ should be significantly more stable than the β one ($Fm\bar{3}c$) for the whole pressure range studied.

A third-order Birch–Murnaghan equation of state (EoS) has been used to parametrize the pressure dependence of the molecular volume of “ $\alpha\text{-Y}(\text{BH}_4)_3$ ” as observed in the experiment, Figure 4. The following EoS parameters have been calculated: $V_0 = 161(6) \text{ \AA}^3$, $B_0 = 25(5) \text{ GPa}$, $B' = 5.25$ (kept constant in the final fit cycle). At first sight the value of bulk modulus (B_0) of $\alpha\text{-Y}(\text{BH}_4)_3$ is not unusual, as it is similar to those typically observed for borohydrides – contained within the limits from 10.9(4) GPa for $\alpha\text{-Mg}(\text{BH}_4)_2$ to 33.8(10) GPa for $\delta\text{-Mn}(\text{BH}_4)_2$.^[20,35] However, it is clear from Figure 4 that above ca. 2 GPa the calculated molecular volume of $\alpha\text{-Y}(\text{BH}_4)_3$ is markedly smaller than the experimental one, with the difference much beyond the typical error of ca. 3 % characteristic for DFT calculations using the GGA

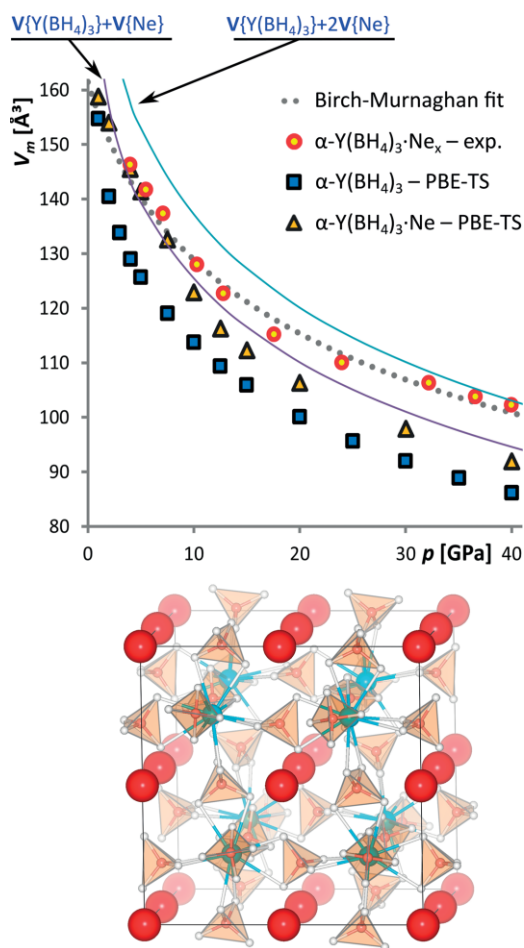


Figure 4. Top: The molecular volume (V_m) of $\alpha\text{-Y}(\text{BH}_4)_3$ and its inclusion compound with neon as a function of pressure – experimental and computed data and the fit of the experimental data to Birch–Murnaghan equation. The lines showing calculated (PBE-TS) sums of $\alpha\text{-Y}(\text{BH}_4)_3$ and Ne volumes have been presented for comparison. Bottom: The crystal unit cell of $\alpha\text{-Y}(\text{BH}_4)_3\cdot\text{Ne}_2$; Ne atoms are shown as the large red spheres.

functionals.^[51] Also, the bulk modulus-governed volume contraction is much more pronounced for the theoretically optimized structure as compared to what is observed in the experiment. The increased volume and larger rigidity of α -Y(BH₄)₃ in our experiment could be readily explained by incorporation of Ne atoms into the structure, as postulated above. In fact, α -Y(BH₄)₃ contains pores of significant volume – at ambient conditions, there are four voids of 35 Å³ in the fractional position 0.5 0.5 0.5 and another four voids of 21 Å³ in the point 0 0 0, as calculated by PLATON software.^[52] At the same time, the calculations based on electron density isosurface of 0.002 au in CrystalExplorer result in a void volume of 211 Å³ per unit cell [i.e. 26.4 Å³ per Y(BH₄)₃ unit], and reveal 3D channels present in the structure, Figure S4.^[53,54] Such voids are sufficient to accommodate Ne atoms, whose extrapolated atomic volume is close to 22 Å³ under ambient pressure, dropping to ca. 16 Å³ during compression to 2 GPa.^[55] At the latter pressure the voids estimated for α -Y(BH₄)₃ (optimized using PBEsol) still reach 19 Å³ per formula unit. Ne might be incorporated because it is a very inert element; indeed, it has been claimed based on theoretical calculations that it is the most inert of all noble gases.^[43–45] For the two lightest noble gases: helium and neon, such inclusion compounds or clathrates have been detected under elevated pressure, e.g. As₄O₆·2He,^[56] Ne_x[NH₄][Fe(HCOO)₃] or Ne_x[NH₄][Ni(HCOO)₃],^[57] clathrate hydrates,^[58] zeolites^[59] or vitreous silica.^[60–62] It is worth to mention, that even larger voids are present in β -Y(BH₄)₃ and its siblings containing larger metal cations, like metastable cubic La(BH₄)₃ or Ce(BH₄)₃.^[14]

The DFT-optimized crystal structure of α -Y(BH₄)₃·Ne_x for $x = 1$ (cf. SI for details) shows much better agreement with the experimental values of molecular volume than the neon-free α -Y(BH₄)₃, especially for the pressures up to ca. 10 GPa, Figure 4. Simultaneously, and despite the rather limited quality of our diffraction data, the additional electronic density from Ne atoms increases the quality of Rietveld fits, Figs. S7–S12. For pressures exceeding 10 GPa the discrepancy between the experimental and theoretical values for α -Y(BH₄)₃·Ne_x ($x = 1$) is larger, which may indicate an even more copious amount of neon into the structure. Our calculations indicate that placing another Ne atom in the larger void, resulting in α -Y(BH₄)₃·Ne_{1.5} stoichiometry, leads to volume expansion of mere 1.4–2.7 % as compared to geometry optimizations of α -Y(BH₄)₃·Ne stoichiometry under the same pressure (cf. SI). On the other hand, double occupation of the smaller void at 0 0 0 results in 10 to 15 % rise in calculated molecular volume. The actual entity formed under high pressure may contain a highly-disordered (“delocalized”) sublattice of Ne atoms due to excessive volume of the voids.

Another important reason for the discrepancy may come from the thermal effects (note, our DFT calculations formally correspond to 0 K and they do not consider the influence of the zero-point motion of atoms on the lattice expansion, while the mobility of weakly-bound inert neon in the structure is supposedly substantial). Regrettably, the sample undergoes progressive amorphization and the data quality does not permit us to unequivocally determine the cause of these discrepancies.

Nevertheless, taken together, the combined experimental and theoretical data suggest the formation of α -Y(BH₄)₃·Ne₁ at lower pressure range with the possible additional incorporation of neon up to α -Y(BH₄)₃·Ne_{1.5} stoichiometry at pressures larger than 10 GPa.

Conclusion

We have investigated α -Y(BH₄)₃ forming a 3D net under gradual compression up to 40 GPa, using Ne as a pressure medium and theoretically, testing several DFT-based approaches. Our results indicate that the used pressure medium strongly influences the processes occurring during compression. Here, we do not detect the phase transition, which was recently reported for this system compressed without pressure medium. Instead we observe incorporation of Ne into the structure, and the product constitutes the first inclusion compound of metal borohydride containing noble gas. At pressures exceeding 10 GPa a gradual amorphization occurs and the Bragg diffraction signals from the sample compressed to 40 GPa are barely visible. The crystallinity is not improved during subsequent decompression to ca. 15 GPa. Our results indicate that dispersion correction (notably PBE-TS approach) is necessary to correctly account for the most stable crystal structures and compressibility of these systems using DFT calculations.

Experimental Section

All the manipulations were performed in the glovebox filled with Ar to avoid decomposition by atmospheric moisture. Y(BH₄)₃ has been prepared via mechanochemical procedure, according to Equation (1): YCl₃ (anhydrous, 99.99 %) and LiBH₄ (> 95 %, both from Sigma-Aldrich) were mixed in ca. 1:3 molar ratio and milled for 60 min in 5 min periods altered with a few minutes rests to avoid overheating. The milling was conducted in vessels containing a single disc (both made of stainless steel) using Laboratory vibrational mill (LMW-S from Testchem, 1400 rpm).^[38,63] Y(BH₄)₃ has been used as synthesized, in a mixture with LiCl (ca. 1:3 molar ratio). It is known that LiCl affects the thermal decomposition of this borohydride,^[5,11] however, we have performed our experiments at room temperature. In fact, the equation of state of LiCl fitted to the data reported here well matches with the previously reported results (SI), therefore LiCl has served as an independent in situ pressure probe.



A small (ca. 50 μm) grain of sample containing both α -Y(BH₄)₃ and LiCl has been loaded on the diamond culet (300 μm), together with Au (99.999 %, Alfa Aesar) pressure probe;^[64] Ne, loaded at ca. 170 MPa has been utilized as a pressure medium. Re gasket, pre-indented to 20 GPa, with ca. 120 μm sample chamber has been used. High-pressure angle-dispersive X-ray diffraction (XRD) measurements have been performed at APS, HPCAT, beamline 16-IDB, $\lambda = 0.4066$ Å. The sample to detector distance and other geometrical parameters were calibrated using CeO₂ standard. Due to a rather weak diffraction from the sample (relatively high background) an accumulation time of up to 240 s has been applied. The two-dimensional diffraction images were analyzed and integrated using the DIOPTAS software.^[65] The most intense single-crystal peaks of Ne were masked before integration. Rietveld refinement of the struc-

Table 1. Comparison of the experimental and theoretical atomic/molecular volumes of Ne (at 5.0 GPa) and $\text{Y}(\text{BH}_4)_3$ at ambient conditions, as calculated using two different functionals with and without dispersion corrections (TS and Grimme). The difference between the calculated and the experimental (exp.) values (Δ) has been given in parentheses.

V/Z [\AA^3] Δ [%]	exp.	PBEsol	PBEsol-TS	PBE	PBE-TS	PBE-Grimme
Ne 5.0 GPa	13.45 ^[55,75]	12.96 (-3.6)	12.83 (-4.6)	13.58 (+1.0)	13.66 (+1.5)	13.18 (-2.0)
α -Y(BH_4) ₃ 1 atm.	159.763 ^[36]	161.37 (+1.0)	155.72 (-2.5)	167.32 (+4.7)	161.54 (+1.1)	162.02 (+1.4)

tures has been performed in Jana2006.^[66] To reach reliable convergence of the refinements, the area of the strongest peak coming from an unidentified impurity has been excluded. A pseudo-Voigt function with Simpson correction for asymmetry has been utilized for modeling of diffraction peak shape. Most of the background has been subtracted before the fit and then fine-corrected using Legendre polynomials. Initially the Rietveld fit of α -Y(BH_4)₃ phase has been attempted to improve using modeling of preferred orientation according to March–Dollase method in the (202) direction. However, the correction appeared unnecessary after model improvement via introducing Ne atoms. Refinement of the α -Y(BH_4)₃Ne_x model does not require correction for preferred orientation. The fractional coordinate of Y atom has been freely refined ($x = y = z$), while (due to limited quality of the diffraction patterns) the BH_4^- anions have been restrained to the geometry of ideal tetrahedra with B–H distances close to 1.1 Å and equal Y–H distances. A third-order Birch–Murnaghan equation of state has been fitted for the data using EoSFit7-GUI program.^[67,68]

Deposition Numbers 433077–433080, for the samples of α -Y(BH_4)₃Ne_x compressed to 4.0, 5.5, 7.1, and 10.3 GPa, respectively contain the supplementary crystallographic data for this paper. These data are provided free of charge by the joint Cambridge Crystallographic Data Centre and Fachinformationszentrum Karlsruhe Access Structures service www.ccdc.cam.ac.uk/structures.

Theoretical optimization of the crystal structures has been performed using density functional theory (DFT), as implemented in CASTEP program^[69] included in the Materials Studio package (Biovia). The generalized gradient approximation (GGA) with ultrasoft pseudopotentials was used. The PBEsol and PBE correlation-exchange functional has been utilized also with Grimme and Tkatchenko–Scheffler (TS) dispersion corrections.^[70–74] As the dispersion correction of PBEsol has not been parametrized by Tkatchenko and Scheffler, the test runs of PBEsol-TS have been parametrized as in ref.^[73] i.e. $s_r = 1.06$, $d = 20.0$. The other approaches used the original parametrizations. Both unit cell parameters and atomic coordinates were optimized using BFGS algorithm. 1000 eV cut-off and a k-point grid density of ca. 0.05 \AA^{-1} were used for final optimizations and calculations of total enthalpy at 0 K. The electronic SCF convergence was 5.0×10^{-7} eV per atom, while the convergence criteria for geometry optimization were as follows: energy change 5.0×10^{-6} eV per atom, max. force 0.01 eV \AA^{-1} , max. stress 0.02 GPa, max. displacement 5.0×10^{-4} Å. The results obtained using various theoretical methods have been compared to the known experimental parameters of crystal structures of Ne and α -Y(BH_4)₃, cf. SI and Table 1. It appeared that the calculations using dispersion-corrected PBE-TS functional in general remain closest to the experimental results, while PBEsol without dispersion corrections is not always able to reproduce the empirical findings. The results obtained using mostly these two approaches were compared.

Acknowledgments

T. J. thanks the Polish Ministry of Science and Higher education for funding (project “Mobility Plus” No. 1064/MOB/13/2014/0).

The experimental work was performed at HPCAT (Sector 16), Advanced Photon Source (APS), Argonne National Laboratory. High-pressure experiments at HPCAT were supported by DOE/BES (DE-FG02-99ER45775). HPCAT operations at the Advanced Photon Source are supported by DOE-NNSA (DE-NA0001974) and DOE-BES (DE-FG02-99ER45775), with partial instrumentation funding by NSF. The Advanced Photon Source is a U.S. Department of Energy (DOE) Office of Science User Facility operated for the DOE Office of Science by Argonne National Laboratory (DE-AC02-06CH11357). T. J. and V. V. S. thank Dr. Ross Hrubciak for the help in the XRD measurements, and Dr. Sergey Tkachev for Ne loading using GSECARS gas loading system at APS. Use of the COMPRES-GSECARS gas loading system was supported by COMPRES under NSF Cooperative Agreement EAR 11-57758 and by GSECARS through NSF grant EAR-1128799 and DOE grant DE-FG02-94ER14466. Dr. P. J. Malinowski is acknowledged for technical help in sample handling. Quantum mechanical calculations were performed at ICM supercomputers within project G29-3. Dr. Pascal Schouwink is thanked for providing details about his experimental studies for bare Y(BH_4)₃ without any pressure medium.

Keywords: Borohydrides · Density functional calculations · High-pressure chemistry · Hydrides · Neon

- [1] W. Grochala, P. P. Edwards, *Chem. Rev.* **2004**, *104*, 1283–1316.
- [2] Q. Lai, M. Paskevicius, D. A. Sheppard, C. E. Buckley, A. W. Thornton, M. R. Hill, Q. Gu, J. Mao, Z. Huang, H. K. Liu, Z. Guo, A. Banerjee, S. Chakraborty, R. Ahuja, K. F. Aguey-Zinsou, *ChemSusChem* **2015**, *8*, 2789–2825.
- [3] M. Paskevicius, L. H. Jepsen, P. Schouwink, R. Černý, D. B. Ravnsbæk, Y. Filinchuk, M. Dornheim, F. Besenbacher, T. R. Jensen, *Chem. Soc. Rev.* **2017**, *46*, 1565–1634.
- [4] H. Hagemann, R. Černý, *Dalton Trans.* **2010**, *39*, 6006.
- [5] M. B. Ley, M. Paskevicius, P. Schouwink, B. Richter, D. A. Sheppard, C. E. Buckley, T. R. Jensen, *Dalton Trans.* **2014**, *43*, 13333–13342.
- [6] B. Richter, J. B. Grinderslev, K. T. Møller, M. Paskevicius, T. R. Jensen, *Inorg. Chem.* **2018**, *57*, 10768–10780.
- [7] T. Jaroń, P. A. Orłowski, W. Wegner, K. J. Fijałkowski, P. J. Leszczyński, W. Grochala, *Angew. Chem. Int. Ed.* **2015**, *54*, 1236–1239; *Angew. Chem.* **2015**, *127*, 1252.
- [8] A. Starobrat, M. J. Tyszkiewicz, W. Wegner, D. Pancierz, P. A. Orłowski, P. J. Leszczyński, K. J. Fijałkowski, T. Jaroń, W. Grochala, *Dalton Trans.* **2015**, *44*, 19469–19477.
- [9] R. Černý, Y. Filinchuk, *Z. Kristallogr. - Cryst. Mater.* **2011**, *226*, 882–891.
- [10] A. Starobrat, T. Jaroń, W. Grochala, *Dalton Trans.* **2019**, *48*, 11829–11837.
- [11] K. Park, H.-S. Lee, A. Remhof, Y.-S. Lee, Y. Yan, M.-Y. Kim, S. J. Kim, A. Züttel, Y. W. Cho, *Int. J. Hydrogen Energy* **2013**, *38*, 9263–9270.
- [12] H. Maekawa, M. Matsuo, H. Takamura, M. Ando, Y. Noda, T. Karahashi, S. I. Orimo, *J. Am. Chem. Soc.* **2009**, *131*, 894–895.
- [13] T. Mezaki, Y. Kuronuma, I. Oikawa, A. Kamegawa, H. Takamura, *Inorg. Chem.* **2016**, *55*, 10484–10489.
- [14] M. B. Ley, M. Jørgensen, R. Černý, Y. Filinchuk, T. R. Jensen, *Inorg. Chem.* **2016**, *55*, 9748–9756.
- [15] M. Brighi, P. Schouwink, Y. Sadikin, R. Černý, *J. Alloys Compd.* **2016**, *662*, 388–395.

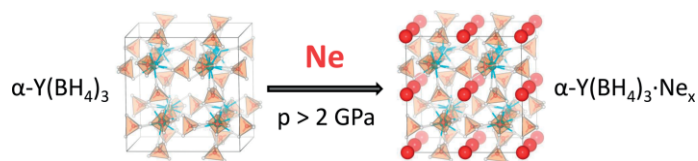
- [16] W. Grochala, T. Jaron, W. Wegner, D. Pancerz, *Acta Crystallogr., Sect. A Found. Adv.* **2014**, *70*, C275–C275.
- [17] W. Wegner, J. van Leusen, J. Majewski, W. Grochala, P. Kögerler, *Eur. J. Inorg. Chem.* **2019**, *2019*, 1776–1783.
- [18] P. Schouwink, E. Didelot, Y.-S. Lee, T. Mazet, R. Černý, *J. Alloys Compd.* **2016**, *664*, 378–384.
- [19] P. Schouwink, M. B. Ley, A. Tissot, H. Hagemann, T. R. Jensen, L. Smrčok, R. Černý, *Nat. Commun.* **2014**, *5*, 5706.
- [20] Y. Filinchuk, B. Richter, T. R. Jensen, V. Dmitriev, D. Chernyshov, H. Hagemann, *Angew. Chem. Int. Ed.* **2011**, *50*, 11162–11166; *Angew. Chem.* **2011**, *123*, 11358.
- [21] E. A. Nickels, M. O. Jones, W. I. F. David, S. R. Johnson, R. L. Lowton, M. Sommariva, P. P. Edwards, *Angew. Chem. Int. Ed.* **2008**, *47*, 2817–2819; *Angew. Chem.* **2008**, *120*, 2859.
- [22] D. Ravnsbaek, Y. Filinchuk, Y. Cerenius, H. J. Jakobsen, F. Besenbacher, J. Skibsted, T. R. Jensen, *Angew. Chem. Int. Ed.* **2009**, *48*, 6659–6663; *Angew. Chem.* **2009**, *121*, 6787.
- [23] P. Schouwink, Investigations on the Structure and Properties of Novel Mixed-Metal Borohydrides, Univ. Genève, **2014**.
- [24] B. Richter, D. B. Ravnsbæk, M. Sharma, A. Spyrtou, H. Hagemann, T. R. Jensen, *Phys. Chem. Chem. Phys.* **2017**, *19*, 30157–30165.
- [25] I. Dovgaliuk, V. Ban, Y. Sadikin, R. Černý, L. Aranda, N. Casati, M. Devillers, Y. Filinchuk, *J. Phys. Chem. C* **2014**, *118*, 145–153.
- [26] J. J. Vajo, S. L. Skeith, F. Mertens, *J. Phys. Chem. B* **2005**, *109*, 3719–3722.
- [27] D. T. Shane, R. L. Corey, C. McIntosh, L. H. Rayhel, R. C. Bowman, J. J. Vajo, A. F. Gross, M. S. Conradi, *J. Phys. Chem. C* **2010**, *114*, 4008–4014.
- [28] T. Jaroń, W. Koźmiński, W. Grochala, *Phys. Chem. Chem. Phys.* **2011**, *13*, 8847–8851.
- [29] J. Nylén, T. Sato, E. Soignard, J. L. Yarger, E. Stoyanov, U. Häussermann, *J. Chem. Phys.* **2009**, *131*, 104506.
- [30] Y. Filinchuk, D. Chernyshov, A. Nevidomskyy, V. Dmitriev, *Angew. Chem. Int. Ed.* **2008**, *47*, 529–532; *Angew. Chem.* **2008**, *120*, 539.
- [31] Y. Filinchuk, A. V. Talyzin, H. Hagemann, V. Dmitriev, D. Chernyshov, B. Sundqvist, *Inorg. Chem.* **2010**, *49*, 5285–5292.
- [32] L. George, V. Drozd, S. K. Saxena, E. G. Bardaji, M. Fichtner, *J. Phys. Chem. C* **2009**, *113*, 15087–15090.
- [33] X. Li, Y. Huang, S. Wei, D. Zhou, Y. Wang, X. Wang, F. Li, Q. Zhou, B. Liu, X. Huang, T. Cui, *J. Phys. Chem. C* **2018**, *122*, 14272–14276.
- [34] S. Nakano, H. Fujihisa, H. Yamawaki, T. Kikegawa, *J. Phys. Chem. C* **2015**, *119*, 3911–3917.
- [35] N. A. Tumanov, E. Roedern, Z. Łodziana, D. B. Nielsen, T. R. Jensen, A. V. Talyzin, R. Černý, D. Chernyshov, V. Dmitriev, T. Palasyuk, Y. Filinchuk, *Chem. Mater.* **2016**, *28*, 274–283.
- [36] C. Frommen, N. Aliouane, S. Deledda, J. E. Fonnelløp, H. Grove, K. Lieutenant, I. Llamas-Jansa, S. Sartori, M. H. Sørbj, B. C. Hauback, *J. Alloys Compd.* **2010**, *496*, 710–716.
- [37] T. Sato, K. Miwa, Y. Nakamori, K. Ohoyama, H. W. Li, T. Noritake, M. Aoki, S. I. Towata, S. I. Orimo, *Phys. Rev. B* **2008**, *77*, 104114.
- [38] T. Jaroń, W. Grochala, *Dalton Trans.* **2010**, *39*, 160–166.
- [39] W. Wegner, T. Jaroń, W. Grochala, *Int. J. Hydrogen Energy* **2014**, *39*, 20024–20030.
- [40] W. Wegner, T. Jaroń, W. Grochala, *J. Alloys Compd.* **2018**, *744*, DOI <https://doi.org/10.1016/j.jallcom.2018.02.020>.
- [41] J. B. Grinderslev, K. T. Møller, M. Bremholm, T. R. Jensen, *Inorg. Chem.* **2019**, *58*, 5503–5517.
- [42] D. B. Ravnsbaek, Y. Filinchuk, R. Černý, M. B. Ley, D. Haase, H. J. Jakobsen, J. Skibsted, T. R. Jensen, *Inorg. Chem.* **2010**, *49*, 3801–3809.
- [43] W. Grochala, *Pol. J. Chem.* **2009**, *83*, 87–122.
- [44] W. Grochala, *Phys. Chem. Chem. Phys.* **2012**, *14*, 14860.
- [45] P. Szarek, W. Grochala, *J. Phys. Chem. A* **2015**, *119*, 2483–2489.
- [46] N. Schouwink, P. Tumanov, ESRF Report, Experiment No: 01–02–1023, Framework and Molecular Metal Borohydrides: High Pressure Studies Assisted by Metal Oxides Analogy, **2014**.
- [47] R. Černý, P. Schouwink, *Acta Crystallogr., Sect. B Struct. Sci. Cryst. Eng. Mater.* **2015**, *71*, 619–640.
- [48] W. Grochala, R. Hoffmann, J. Feng, N. W. Ashcroft, *Angew. Chem. Int. Ed.* **2007**, *46*, 3620–3642; *Angew. Chem.* **2007**, *119*, 3694.
- [49] Y. S. Lee, J. H. Shim, Y. W. Cho, *J. Phys. Chem. C* **2010**, *114*, 12833–12837.
- [50] J. P. Perdew, Y. Wang, *Phys. Rev. B* **1992**, *45*, 13244–13249.
- [51] P. Haas, F. Tran, P. Blaha, *Phys. Rev. B* **2009**, *79*, 085104.
- [52] A. L. Spek, *Acta Crystallogr., Sect. D Biol. Crystallogr.* **2009**, *65*, 148–155.
- [53] M. A. S. M. J. Turner, J. J. McKinnon, S. K. Wolff, D. J. Grimwood, P. R. Spackman, D. Jayatilaka, **2017**.
- [54] M. J. Turner, J. J. McKinnon, D. Jayatilaka, M. A. Spackman, *CrystEngComm* **2011**, *13*, 1804–1813.
- [55] A. Dewaele, F. Datchi, P. Loubeyre, M. Mezouar, *Phys. Rev. B* **2008**, *77*, 094106.
- [56] P. A. Guńka, K. F. Dziubek, A. Gładysiak, M. Dranka, J. Piechota, M. Hanfland, A. Katrusiak, J. Zachara, *Cryst. Growth Des.* **2015**, *15*, 3740–3745.
- [57] I. E. Collings, E. Bykova, M. Bykov, S. Petitgirard, M. Hanfland, D. Paliwoda, L. Dubrovinsky, N. Dubrovinskaia, *ChemPhysChem* **2016**, *17*, 3369–3372.
- [58] D. Londono, J. L. Finney, W. F. Kuhs, *J. Chem. Phys.* **1992**, *97*, 547–552.
- [59] Y. Lee, J. A. Hriljac, T. Vogt, *J. Phys. Chem. C* **2010**, *114*, 6922–6927.
- [60] G. Shen, Q. Mei, V. B. Prakapenka, P. Lazor, S. Sinogeikin, Y. Meng, C. Park, *Proc. Natl. Acad. Sci. USA* **2011**, *108*, 6004–6007.
- [61] C. Weigel, A. Polian, M. Kint, B. Rufflé, M. Foret, R. Vacher, *Phys. Rev. Lett.* **2012**, *109*, 245504.
- [62] C. Weigel, M. Foret, B. Hehlen, M. Kint, S. Clément, A. Polian, R. Vacher, B. Rufflé, *Phys. Rev. B* **2016**, *93*, 224303.
- [63] T. Jaroń, W. Wegner, K. J. Fijałkowski, P. J. Leszczyński, W. Grochala, *Chem. Eur. J.* **2015**, *21*, 5689–5692.
- [64] Y. Fei, A. Ricolleau, M. Frank, K. Mibe, G. Shen, V. Prakapenka, *Proc. Natl. Acad. Sci. USA* **2007**, *104*, 9182–9186.
- [65] C. Prescher, V. B. Prakapenka, *High Pressure Res.* **2015**, *35*, 223–230.
- [66] V. Petříček, M. Dušek, L. Palatinus, V. Petříček, M. Dušek, L. Palatinus, *Z. Kristallogr. - Cryst. Mater.* **2014**, *229*, 345–352.
- [67] R. J. Angel, J. Gonzalez-Platas, M. Alvaro, *Z. Kristallogr. - Cryst. Mater.* **2014**, *229*, 405–419.
- [68] J. Gonzalez-Platas, M. Alvaro, F. Nestola, R. Angel, *J. Appl. Crystallogr.* **2016**, *49*, 1377–1382.
- [69] S. J. Clark, M. D. Segall, C. J. Pickard, P. J. Hasnip, M. I. J. Probert, K. Refson, M. C. Payne, *Z. Kristallogr.* **2005**, *220*, 567–570.
- [70] J. P. Perdew, K. Burke, M. Ernzerhof, *Phys. Rev. Lett.* **1996**, *77*, 3865–3868.
- [71] J. P. Perdew, A. Ruzsinszky, G. I. Csonka, O. A. Vydrov, G. E. Scuseria, L. A. Constantin, X. Zhou, K. Burke, *Phys. Rev. Lett.* **2008**, *100*, 136406.
- [72] E. R. McNellis, J. Meyer, K. Reuter, *Phys. Rev. B* **2009**, *80*, 205414.
- [73] W. A. Al-Saidi, V. K. Voora, K. D. Jordan, *J. Chem. Theory Comput.* **2012**, *8*, 1503–1513.
- [74] M. Fischer, R. J. Angel, *J. Chem. Phys.* **2017**, *146*, 174111.
- [75] D. N. Batchelder, D. L. Losee, R. O. Simmons, *Phys. Rev.* **1967**, *162*, 767–775.

Received: July 1, 2020

Metal Borohydrides

T. Jaroń,* A. Starobrat,
V. V. Struzhkin, W. Grochala 1–7

Inclusion of Neon into an Yttrium Borohydride Structure at Elevated Pressure – An Experimental and Theoretical Study



During compression in neon, the cage-like structure of $\alpha\text{-Y}(\text{BH}_4)_3$ is stabilized by inclusion of Ne into the available voids at 0.5 0.5 0.5 and 0 0 0. The inclusion compound preserves high

crystallinity up to ca. 10 GPa, while gradual amorphization is observed at higher pressures. Using dispersion correction (PBE-TS) is necessary for proper DFT-based modeling of this system.

doi.org/10.1002/ejic.202000631